ISSN 0361-5219, Solid Fuel Chemistry, 2024, Vol. 58, No. 4, pp. 337–346. © Allerton Press, Inc., 2024.

Analysis of the Natural Hazard of the Mining Void Zone Based on Incomplete Collapse of the Roadway in the Return Mining

Zongxiang Li[a,b], Wenshuo Sun[a,b,*], Dongjie Hu[a,b], and Yuhang Li[a,b]

[a] *College of Safety Science and Engineering, Liaoning Technical University, Fuxin Liaoning, 123000 China*

[b] *Key Laboratory of Mine Thermodynamic Disasters and Control of Ministry of Education, Liaoning Technical University, Fuxin Liaoning, 123000 China*

** e-mail: sunws3910@163.com*

Received January 4, 2024; revised January 16, 2024; accepted April 10, 2024

Abstract—Determining the risk of spontaneous combustion of coal remains in the airspace is crucial to the safe production of mines. Therefore, to investigate the danger of spontaneous combustion in the airspace when the overlying rock layer is not sufficiently compacted, the 1304 working face of Hongyang no. 2 Mine was taken as the research object. The experimental device was developed to measure the oxygen consumption rate, and the negative exponential function model was used to analyze the change rule of the oxygen volume fraction of the coal samples. Combined with a large amount of measured data of the working face and the change of the wind speed of the inlet and return tunnel, a CFD model of the ground without subsidence of the bubbling medium of the mining airspace was established, and numerical simulation was carried out on the flow field of the working face's airspace area by using FLUENT software to get the oxygen volume fraction distribution law of the airspace area distribution law. The results show that the continuous oxygen consumption rate of the coal sample is $\gamma = 9.3381 \times 10^{-7}$ mol/(m^3 s). Then, the oxygen volume fraction of choking (critical) under the actual temperature is 14.4%. The maximum range of the spontaneous combustion oxidation zone in the goaf is 25 to 176 m away from the working face. The work safety advancement rate is 1.86 m/d, and the actual advancement speed is 9.6 m/d, which also presents a lower risk of spontaneous combustion. The on-site test data matches well with the simulation results, which verifies the validity of the simulation and provides a basis for the prevention and control of spontaneous combustion of the coal left in the mining area to ensure the safe production of the mine.

Keywords: coal mine safety, spontaneous combustion of residual coal, closed oxygen consumption test, spontaneous combustion oxidation zone, safe propulsion speed, Computational Fluid Dynamics (CFD) simulation

DOI: 10.3103/S0361521924700228

1. INTRODUCTION

The spontaneous combustion of residual coal in goaf poses a great threat to human health and safety production in underground coal mines [1–3]. Numerous scholars have conducted in-depth studies on the mechanism of spontaneous coal combustion and the influence of oxygen volume fraction distribution on spontaneous combustion in the airspace zone [4–6]. Xu et al. quantitatively analyzed the division of three zones in the mining airspace from the theoretical point of view. They put forward the concept of the minimum safe propulsion speed and its calculation method, which laid the foundation for the subsequent prediction and forecasting of fire in the mining airspace [7]. Yu et al. proposed the "three zones" of spontaneous combustion in the air mining area from the automatic combustion mechanism and danger. They used the data processing methods of the mean smoothing method and primary exponential smoothing method to obtain the results of the spontaneous combustion "three zones" division [8]. Gui et al. analyzed spontaneous coal combustion's characteristic temperature and index gas through the program heating experiment, which provided the basis for dividing spontaneous combustion into "three zones" in the Y-type ventilation mode [9]. In addition, many other scholars have given the results of the division and risk assessment of spontaneous combustion "three zones" in the mining airspace under the working face with different characteristics by using on-site test data and simulation analysis of application software [10–12]. Wang et al. for multi-jacketed top slab generalized mining face [13], Chen et al. for large-height generalized mining face [14], Zhuo et al. for shallow buried coal beds [15], and Su et al. for sharply inclined longwall face (50° inclination angle) [16]. All of the above

have explored the relevant laws under many specific conditions and have determined the methods for judging the risk of spontaneous combustion of coal remains in the air-mining zone, which provided a reference for the production in similar engineering environments.

However, in practical engineering, the oxygen volume fraction of 8 or 10% is usually used as the basis for delineating the spontaneous combustion oxidation zone. However, there is a big difference in the coal beds between different mines, and the geological conditions and mining techniques are other. For different coals or coal types, the oxidizing activity of the coal is different, the spontaneous combustion characteristics are different, and the related values such as the oxygen consumption rate, the continuous oxygen consumption rate of the coal samples, and the critical volume fraction of oxygen consumption in the asphyxiation zone are also different [17–20]. Therefore, the volume fraction of 8 or 10% oxygen was used as the boundary between the oxidation heating zone and the asphyxiation zone, which can only be used as a general reference. That is to say, this kind of "one-size-fits-all" approach can not meet the situation of the actual production of different coals, and it is not enough to accurately portray the distribution of the "three zones" in the mining zone under specific conditions. Then it can not accurately evaluate. It is not enough to accurately characterize the distribution of the "three zones" in the mining area under particular conditions. It thus cannot accurately assess the spontaneous combustion risk of the mining area under specific conditions.

Therefore, this paper focuses on the 1304 working face in the west-third lower mining area of Hongyang no. 2 Mine, where the roof plate of the overlying old air zone is incompletely collapsed. A leakage channel is formed in the mining air zone. According to the theory of field flow, as the leakage flow moves through the mining air zone, oxygen will be continuously consumed, causing oxygen depletion along the wind flow path [21–23]. To explore the distribution of the "three belts" of the spontaneous combustion of the mining air zone in the case of the increase of the leakage power, we apply the closed depletion method to determine the distribution of the "three belts" of spontaneous combustion. To investigate the distribution of spontaneous combustion in the air mining zone under the condition of enhanced wind leakage power, the oxygen consumption rate of coal samples from the 13# coal seam of Hongyang no. 2 Mine is measured by the closed oxygen consumption experiment to determine the oxygen volume fraction of choking (critical) under the actual temperature, and the CFD model of the fallout medium of the ground unsinkable air mining zone is established. Based on the "O" ring theory [24] and combined with the field measurement data, the UDF control program is written to debug the distribution of the fallout medium in the mining area, and the simulation is carried out by using ANSYS FLUENT software to compare and validate the on-site observation results. The critical safety advancement degree is further calculated to guide the work of fire prevention and extinguishing in the mining area.

2. RESEARCH METHOD

2.1. Closed Oxygen Consumption Experimental System

In order to obtain the oxygen consumption rate of coal samples under continuously varying oxygen concentrations, the research team specially developed a closed oxygen consumption experimental apparatus. The schematic and physical representation of the apparatus can be seen in Fig. 1. The experiment employed a closed oxygen consumption method [25], in which the coal sample was enclosed in a container. The air inside the container was circulated and brought into sufficient contact with the coal sample using an air pump. As the experiment proceeded, the coal sample underwent continuous oxidation, leading to a depletion of oxygen in the container. The volumetric fraction of oxygen inside the container was monitored and recorded in real-time, and the oxygen consumption rate gradually stabilized [26]. Based on the characteristic pattern of oxygen concentration variations during the coal-oxygen consumption process inside the experimental container, the desired parameters were indirectly obtained [27, 28].

2.2. Engineering Field Measurement

The 13th coal seam in the lower part of the West 3rd panel in Hongyang Mine is composite. The length of the 1304 working face in this area is approximately 1060 m, with an average seam thickness of 2.7 m and an average dip angle of 5°. The inclined longwall retreat mining method is adopted, and a U-shaped ventilation system is used for the working face. Currently, the length of the 1304 working face is 94 m, with an advance rate of 0.8 m per cycle and a production rate of 9.6 m per day. The intake air volume for the working face is 1214 cubic meters per minute. The 13th coal seam is prone to spontaneous combustion and has stable deposition with well-developed strata and joints. The 12th coal seam has already been fully mined, and it is situated on top of the 13th coal seam, with an average separation distance of 2 m. This forms the re-generated roof of the 13th coal seam, which is connected to the old gob area and allows gas communication. The spontaneous combustion period of the coal seam is estimated to be between 92 and 230 days. The 12th coal seam above has the shortest spontaneous combustion period of 81 days. During the mining process, the coal residues from the 12th coal seam above and the floating coal left from the 13th coal seam combine to form a spontaneous combustion hazard in the goaf area. Due to the use of U-shaped steel shed support during transportation and backfilling, the incomplete filling of the corners will enhance

(a) Experimental device structure diagram

(b) The physical diagram of the experimental device

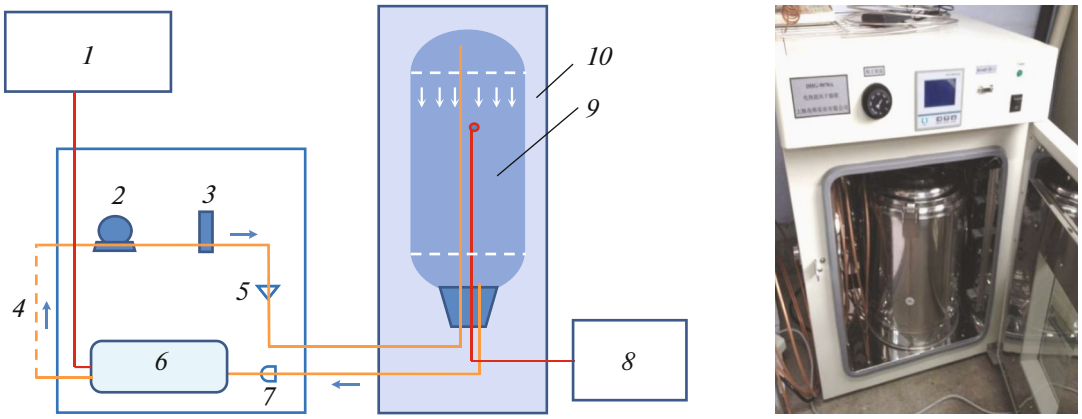

Fig. 1. Coal sample closed oxygen consumption experimental device diagram structure diagram and physical diagram: *1* – computer and data acquisition module. *2* – air pump, *3* – flow meter, *4* – sealed tube; *5* – check valve, *6* – detection chamber, *7* – filter, *8* – electronic temperature measurement, *9* – coal sample tank, *10* – thermostat.

the air leakage effect in the goaf area and increase the risk of spontaneous combustion of the coal residues in the goaf area [29].

According to the ground temperature measurement report during the field exploration, the 13th coal seam at a depth of 850 m is classified as a secondary heat hazard zone (37°C). The current elevation of the return airway of the working face is –836.23 m, and the intake airway elevation is –850.11 m. The temperature of the goaf area near the working face during mining is approximately 33°C. Based on long-term observations, it has been determined that the total gas emission from the working face and goaf area is relatively low. Therefore, the influence of gas emissions on the oxygen concentration distribution in the goaf area is not considered.

Within the goaf area, gas composition is monitored using a bundled tube, which also facilitates the measurement of internal temperature. This provides direct insights into the natural environmental changes within the goaf area and the temperature increase caused by residual coal oxidation. These data serve as the basis for the computer numerical simulation to delineate the "spontaneous combustion zones" in the goaf of the 13th coal seam in the lower part of the West 3rd panel and to determine the natural hazard areas as well as assess the spontaneous combustion risk at the working face.

The return airway side of the goaf area is a key area for studying the inflow of harmful gases produced from gas and coal oxidation into the working face. The working face leaks air into the goaf area on the intake side at the lower part of the goaf, promoting the coal oxidation process. This region is a key area for studying the maximum width of the spontaneous combustion oxidation zone. In the initial stage, the length of the monitoring bundle tube on the intake side is 180 m. The protection tube for the bundle tube is constructed using abandoned grouting and nitrogen injection pipelines, and a dual-core bundle tube with an inner diameter of 10 mm is installed. An artificial sampling station is set up at the end of the bundled tube (far from the working face), taking the return airway side monitoring point 1# as an example. The arrangement of the embedded pipe observation casing and the bundle tube protection device in the goaf area is shown in Fig. 2.

2.3. Study on CFD Simulation of Goaf Flow Field

The coal body's extraction leads to the overlying strata's caving, forming a caving zone. Influenced by the cantilever beam structure, the distribution of caving height in this area can be approximated as a rounded rectangular zone, more prominent near the sides of the goaf and smaller within the compacted stable zone [30]. Above the caving zone, the rock layers show bending and sinking, forming apparent zoned discontinuities [31]. Based on this, a diagram dividing the goaf into three caving zones along the height of the caving is established, as shown in Fig. 3.

Based on the actual parameters of the 1304 working face in the lower part of the West 3rd panel of the Hongyang no. 2 Mine, the actual site is appropriately simplified to establish a ground subsidence-free goaf caving medium CFD model, as shown in Fig. 4. The dimensions are set as follows: the intake airway and return airway measure 30 m in length, 3 m in width, and 3 m in height; the working face measures 94 m in length, 3 m in width, and 3 m in height; the cross-section of the goaf is trapezoidal, with dimensions of 200 m in length, (94 m in width at the bottom + 40 m in width at the top), and 70 m in height. The intersection

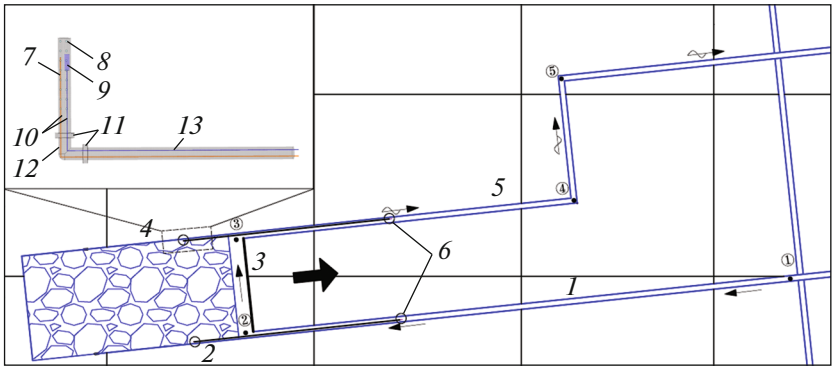

Fig. 2. Arrangement of mining roadway and test boundary along 1304 working face: *1* – intake airway, *2* – inlet air measuring point 1, *3* – working face, *4* – return air measuring point 1, *5* – return airway, *6* – manual sampling point, *7* – gas sampling tube, *8* – air hole, *9* – thermocouple, *10* – bundled tube, *11* – flange joint, *12* – sleeve, *13* – temperature measuring wire.

of the floor and the intake airway corner is chosen as the origin of the coordinate system.

3. RESULTS AND ANALYSIS

3.1. Determine the Suffocated (Critical) Oxygen Volume Fraction

Based on the principle of closed oxygen consumption experiments, oxygen consumption characteristic experiments were conducted on coal samples from the 13th coal seam of the Hongyang no. 2 Mine under a temperature of 30°C. The relationship between oxygen volume fraction and time and the corresponding fitted curve was obtained. Refer to Fig. 5 for details.

It can be observed that during the closed oxygen consumption experiment, as time increases, the volumetric fraction of oxygen, $c(\tau)$, gradually exhibits a significant negative exponential relationship, as follows:

$$c(\tau) = c_b + (c_0 - c_b) \cdot e^{-\lambda_c \tau}. \quad (1)$$

In the equation, c_0 represents the initial volumetric fraction of oxygen, which is taken as 20.45%; λ_c represents the decay rate of the oxygen volumetric fraction, s^{-1}; c_b represents the steady-state value of the oxygen volumetric fraction, %; τ represents the oxidation time, s.

The volumetric oxygen consumption rate of the coal sample container at an oxygen volumetric fraction of c_0 can be represented as follows:

$$\gamma = -0.4464\lambda_c(c_0 - c_b). \quad (2)$$

In the equation, γ represents the volumetric oxygen consumption rate at oxygen concentration c_0, mol/(m^3 s).

Through regression analysis, the decay rate of the oxygen volumetric fraction in the experimental container is determined to be $\lambda_c = -5.4334 \times 10^{-5}$, and the volumetric oxygen consumption rate of the coal sample was calculated to be $\gamma = 9.3381 \times 10^{-7}$ mol/(m^3 s).

From the perspective of oxygen consumption rate, when the oxygen volume fraction of the coal sample is 16.6% under ambient conditions at 30°C, the oxygen consumption rate is prolonged, approaching the criti-

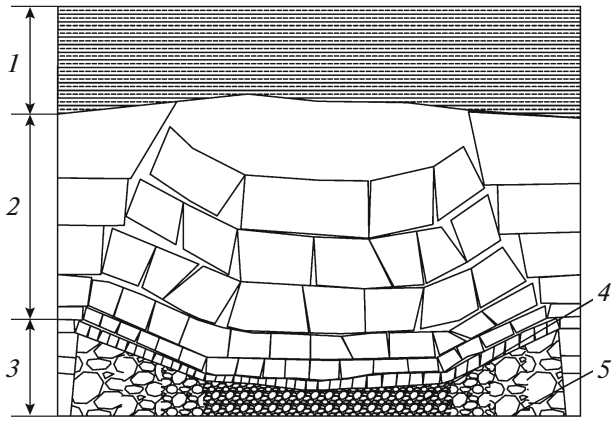

Fig. 3. CFD model diagram of the collapse medium in the subsidence-free goaf: *1* – curved subsidence zone, *2* – fracture zone, *3* – falling zone, *4* – compaction stable zone, *5* – uncompacted stable zone.

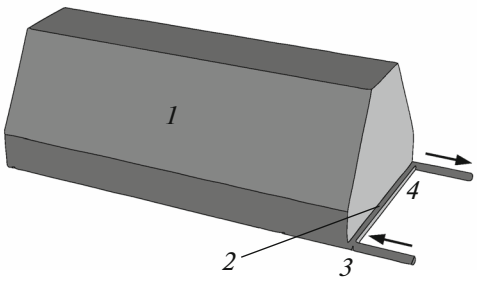

Fig. 4. Ground non-sinking cavity collapse medium cfd model and meshing diagram: *1* – overlying goaf, *2* – 1304 working face, *3* – transportation channel, *4* – return air channel.

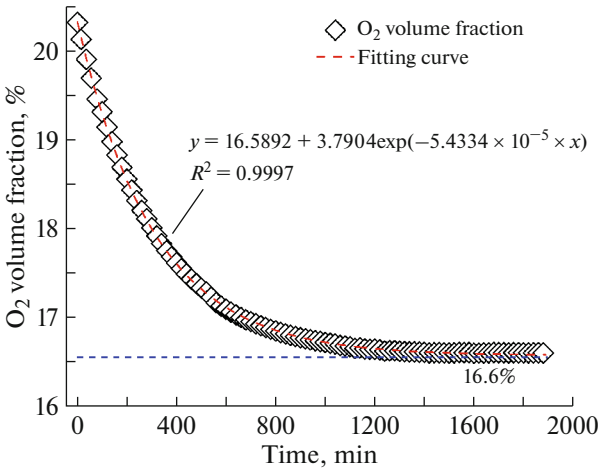

Fig. 5. Data and fitting curve of the oxygen volume fraction over time for coal.

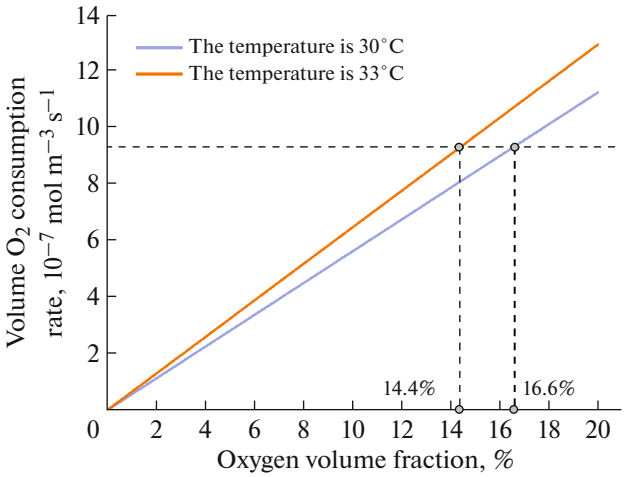

Fig. 6. Relationship between volume oxygen consumption rate and oxygen volume fraction for coal.

cal value. This pattern is consistent with the findings of Wang et al., which indicate that the heat generated by coal oxidation is less than the heat dissipation in the environment [32, 33]. In addition, the value of λ_c directly reflects the strength of the coal sample's oxygen consumption capacity. By comparing and analyzing the coal samples from Dayan Coal Mine (DY) and Hongqingliang Coal Mine (HQL) with the coal samples from Hongyang no. 2 Mine (HY), the characteristic oxygen consumption parameters of different coal samples are shown in Table 1. Comparing the oxygen consumption parameters of the different coal samples at 30°C, it is evident that the volumetric oxygen consumption rate of the HY coal sample is much lower than that of the DY and HQL coal samples. Therefore, under the same conditions, the stable oxygen concentration of the HY coal sample is also higher than that of the other two types of coal samples. The self-ignition capability of the coal sample from Hongyang no. 2 Mine is weaker than the other two types of coal samples with established self-ignition characteristics.

Compared with the Hongqingliang coal sample, both the mass oxygen consumption rate and oxygen volumetric fraction of the coal sample exhibit an exponential increase. Compared to the experimental temperature of 30°C, the mass oxygen consumption rate of coal decreases by approximately 1.5×10^{-8} mol/(kg s) at 20°C, which is half of the value at 30°C. With this proportion in mind, it can be estimated that at an actual temperature of 33°C, the oxygen consumption rate of the coal sample from Hongyang Mine increases by approximately 15%, as shown in Fig. 6. Consequently, a new expression is derived, representing the level of the constant line of volumetric oxygen consumption rate. It can be confirmed that the critical oxygen volume fraction for the strongest smothering (critical) of residual coal in the goaf of the 13th coal seam at 33°C is 14.4%. The above data can provide basic parameters for subsequent simulation studies.

3.2. Analysis of Air Leakage Boundary Conditions in Working Face Stope

In order to conduct a more detailed analysis of the airflow in the goaf, it is necessary to observe the airflow along the working face and the two roadway sections. The boundary points for along-the-route testing (①–⑤) are shown in Fig. 5:

- From the transport roadway (point ①) to the intake corner of the working face (point ②), the length is 1120 m, divided into 89 measurement points.
- After passing through the working face to the return corner (point ③), there is a 94 m section divided into 26 measurement points, with a spacing of 3.5 m.
- From the return corner (point ③) to the return roadway (point ④), there is a 590 m section divided into 60 measurement points.

Table 1. Oxygen consumption characteristic parameters of different coal samples

Coal sample	Coal variety	C_0, %	C_b, %	λ_c, s^{-1}	γ, mol m^{-3} s^{-1}
HY	Lean coal	20.45	16.6145	5.4334×10^{-5}	9.3381×10^{-7}
DY	Brown coal	20.68	8.0315	1.2282×10^{-4}	6.8912×10^{-6}
HQL	Non-caking coal	20.61	7.7161	2.1632×10^{-5}	1.2441×10^{-6}

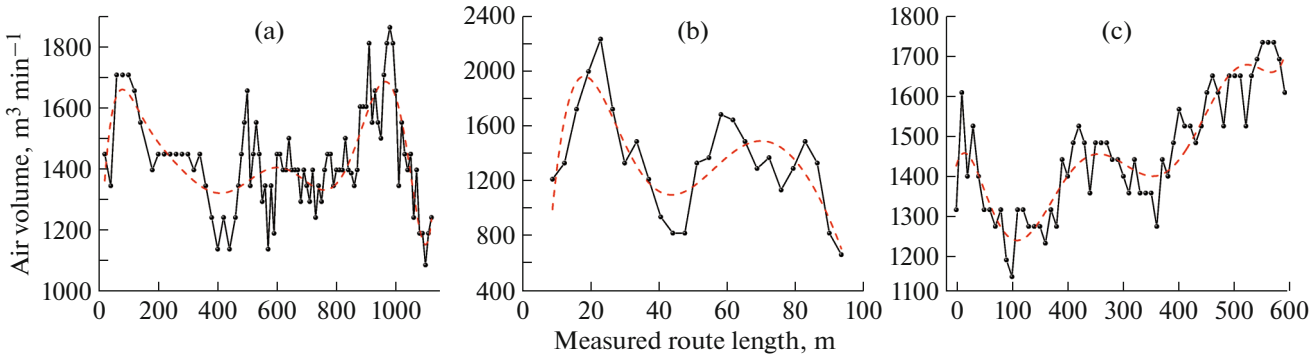

Fig. 7. Measured the wind speed changes along the intake and return airways and the working face.

Based on the abundant on-site measured air volume data from the intake airway, return airway, and working face, plot the profile airflow change curve as shown in Fig. 7.

In Fig. 7a, the *x*-axis represents the distance from the intake roadway to the working face, ranging from 20 to 1140 m. Due to the complexity of the airflow along the route, the accuracy of the wind speed measurements at specific points may be compromised. The continuous decrease in wind speed from 1120 to 1140 m can be attributed to air leakage in the upper goaf area. However, overall, the trend of wind speed variation along the route is apparent and consistent with the actual conditions. This information can be used as a reference for air leakage distribution in CFD simulations.

In Fig. 7b, the measured cross-sectional area of the 1304 mining working face is 9.715 m^2, with an average wind speed of 2.53 m/s. The total air intake volume at the working face is 1442.1 m^3/min. From the observed data in Fig. 8, the three lowest measured values (1204.66, 932.64, 1126.74) are averaged to eliminate noise. This calculation yields a leakage airflow from the working face to the goaf of 272.1 m^3/min, accounting for 18.82% of the working face airflow. This leakage percentage is slightly higher than the general range of 10 to 15% for the working face leakage to the goaf, indicating the validity of the observations. It can be inferred that, under the condition of insufficient roof caving in the two headings, the primary leakage of airflow from the working face to the goaf occurs through the intake corner.

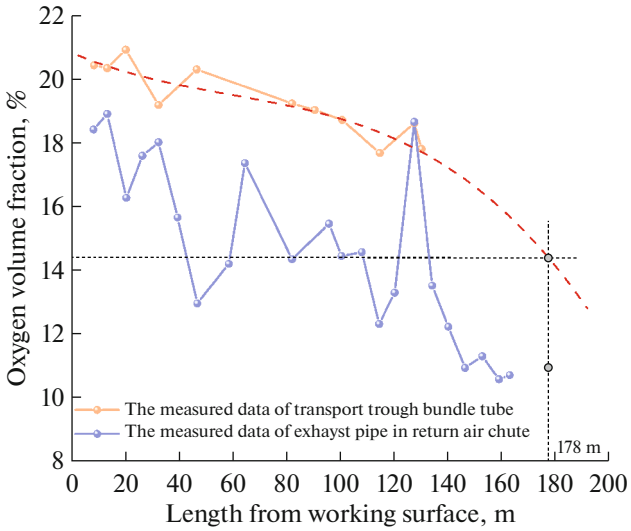

Fig. 8. Observation and prediction results of the oxygen volume fraction on the intake and return air side in the goaf.

Figure 7c shows that the wind speed gradually decreases along the route from the return end of the working face to the end of the return airway. Within a range of 220 m from the return end of the working face, the wind speed decreases rapidly due to air leakage in the upper goaf, which is consistent with the actual situation. Within the 340 to 550 m range, there is a significant air leakage and return flow from the caving area of the overlying #12 coal seam, resulting in an increasing airflow in the roadway. This indicates the existence of air leakage in the caving area of the overlying #12 coal seam in the 1304 working face, where the airflow flows from the intake roadway through the caving area and returns to the return airway, leading to a noticeable increase in the airflow in the return section.

It can be concluded that premature air leakage communication exists between the intake roadway and return airway of the 1304 working face through the caving area of the overlying #12 coal seam, with an estimated leakage airflow of approximately 200 m^3/min. This suggests an oxygen supply to the caving area of the overlying #12 coal seam. The latest identification of the remaining coal in the #12 coal seam indicates that it is not prone to spontaneous combustion and has a low coal oxidation capacity. Thus, there have been no signs of self-ignition in the actual engineering practice.

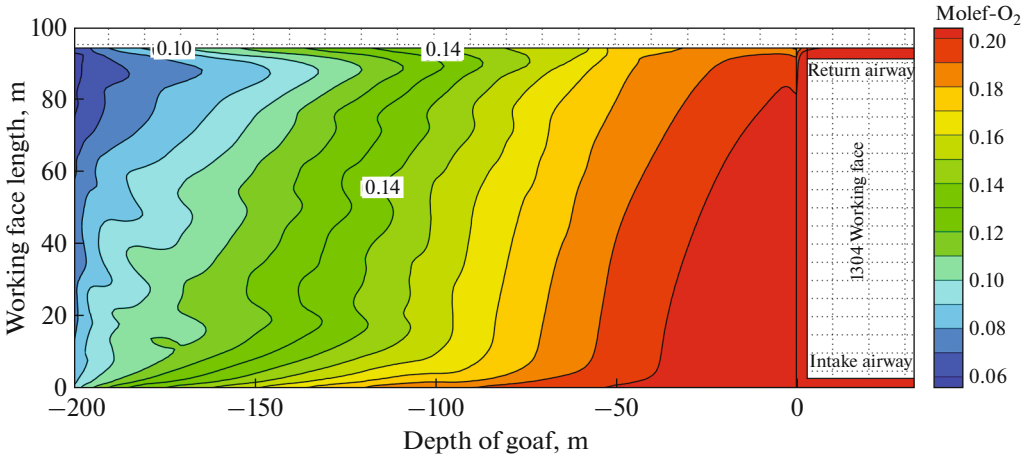

Fig. 9. The oxygen volume fraction distribution of the oxygen-consuming layer of the left coal in the goaf $z = 0.5$ m.

3.3. Analysis of Measured Oxygen Volume Fraction in Goaf

Based on the measurements from the borehole monitoring, the data of the oxygen volumetric fraction within a range of 135 m on the intake side and 160 m on the return side of the goaf in the 1304 working face are shown in Fig. 8. Fit the oxygen volume fractions on the intake and return sides separately with the burial depth of the sampling head, the relationship between the measured oxygen volumetric fraction ***y*** in the goaf on the intake side and the distance ***x*** from the working face is determined:

$$y = 20.91 - 0.037x + 3.630\times10^{-4}x^2 - 2.026\times10^{-6}x^3. \quad (3)$$

Assuming that the decreasing trend of the oxygen volumetric fraction on the return side approximately follows a linear relationship, the relationship between the measured oxygen volumetric fraction **y'** in the goaf on the return side and the distance **x'** from the working face is obtained:

$$y' = 18.31 - 0.04x'. \quad (4)$$

In equation, **y** and **y'** represent the values of the oxygen volumetric fraction in the goaf, %; **x** and **x'** represent the distance from the working face, m.

Based on the above equation, by calculation, the boundary position of the goaf on the intake side, where the oxygen volumetric fraction reaches the quenching (critical) value (14.4%) obtained from closed oxygen consumption experiments, is at **x** = 95 m. Similarly, it can be calculated that when the oxygen volumetric fraction is 14.4% on the intake side, the position from the working face is at **x'** = 178 m, and the predicted oxygen concentration in the goaf on the return side at a distance of 178 m from the working face is 10.8%.

As the distance from the working face increases, the oxygen concentration in the goaf gradually decreases. However, the oxygen distribution changes gradually due to insufficient air leakage in the intake-side roadway. In addition, one of the reasons for the generally high oxygen concentration in the goaf is coal's weak oxygen consumption capacity. Furthermore, the gas has been adequately released during the extraction of the top coal, resulting in low gas content and relatively high oxygen concentration.

3.4. Determination of Spontaneous Combustion Oxidation Zone Width in Goaf

According to the division law of three zones of height caving, a specific UDF control program is developed to control the distribution of the caving medium in the goaf. The distribution of the oxygen volume fraction field in the goaf has been obtained. A plane with a height of 0.5 m is established to represent the distribution of oxygen volume fraction in the residual coal consumption layer in the goaf, as shown in Fig. 9. The 14.4% oxygen volume fraction curve is approximately 178 m from the working face. At this point, the corresponding oxygen volume fraction on the return air side of the goaf is approximately 10.5%, which is consistent with the observed and predicted data of the oxygen volume fractions on both the intake and return air sides of the goaf, validating the accuracy of the results.

According to the analysis of the higher range of oxygen concentration and the on-site fiber-optic temperature measurement results, the range of the cooling zone behind the working face is determined to be at a distance of 25 m from the working face. Simulation results show that the goaf's self-ignition oxidation heating zone has a wedge-shaped distribution, ranging from 25 to 176 m behind the working face, with a maximum width (L_m) of 151 m [34]. The division of the self-ignition hazard zone is shown in Fig. 10. This validates the accuracy of the prediction results based on the measured data.

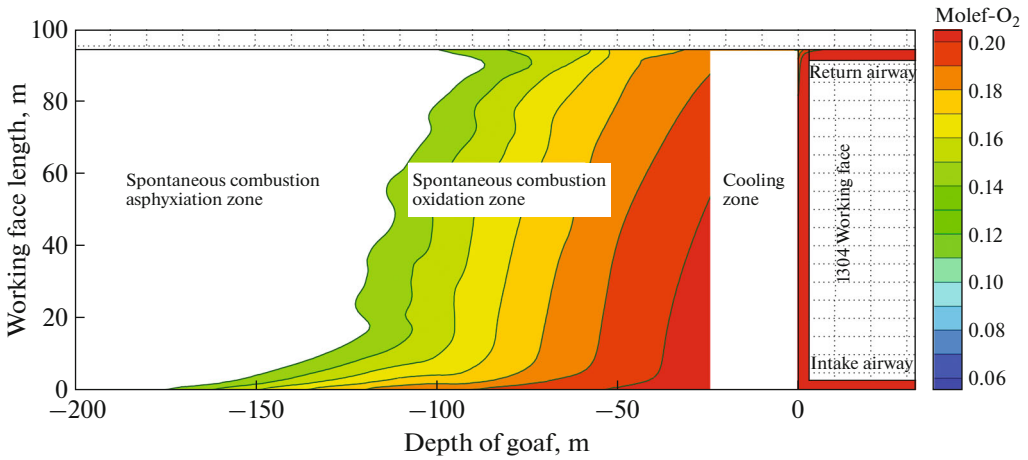

Fig. 10. Oxygen volume fraction distribution and spontaneous combustion danger zone division.

4. ANALYSIS OF THE RISK AND SAFETY OF SPONTANEOUS COMBUSTION IN GOAF OF 1304 WORKING FACE

The maximum width of the spontaneous combustion oxidation zone for the 1304 working face is L_m = 151 m. Based on the current mining advance rate of 9.6 m/d, the remaining coal spontaneous combustion oxidation time in the goaf can be calculated as follows:

$$\tau_1 = \frac{L_m}{v_1} = \frac{151}{9.6} = 15.73 \text{ d} < 81 \text{d}. \quad (5)$$

In equation, L_m represents the width of the spontaneous combustion oxidation zone in the goaf, m. v_1 denotes the advancing rate of the working face, m/d. τ_1 represents the maximum time for spontaneous combustion oxidation heating, d. τ_1^* stands for the earlier and shortest natural ignition period. The possibility of residual coal from the overlying no. 12 coal seam in the goaf is considered, so the relatively shorter natural combustion period of 81 days for no. 12 coal seam is used for calculation.

The goaf is considered safe when Eq. (3) relationship is satisfied. Otherwise, there is a certain level of risk for spontaneous combustion in the goaf. The term "spontaneous combustion risk" here refers to the possibility of spontaneous combustion occurring in the remaining coal in the goaf. However, it does not imply that spontaneous combustion will happen. This is because the earlier and shortest natural ignition period τ_1^* is determined under conditions most favorable for coal spontaneous combustion (either through experimental measurements or historical data from the site). The actual coal spontaneous combustion environment in the field may not be as favorable, as it is influenced by various factors, particularly factors such as mine water injection and a low amount of residual coal floater.

Therefore, the minimum safe advancing rate (or critical advancing rate v_1^*) for the current stage of the 1304 working face is obtained as follows:

$$v_1^* = \frac{L_m}{\tau_1^*} = \frac{151}{81} = 1.86 \text{ m/d}. \quad (6)$$

The so-called minimum safe advancing rate of the working face does not mean a risk of spontaneous combustion if the advancing rate is less than 1.86 m/d for one or several instances. Instead, it indicates a risk of spontaneous combustion when the cumulative average advancing rate is less than 1.91 m/d within an accumulated period of 81 days.

Therefore, under the current conditions of the U-shaped ventilation arrangement and the absence of fire prevention measures in the 1304 working face of the Hongyang no. 2 Mine, there is no risk of spontaneous combustion in the goaf when the daily advancing rate is 9.6 m/d.

5. CONCLUSIONS

(1) The application of closed oxygen consumption experiments to determine the critical oxygen volume fraction of different coal types is reliable and feasible. This method can more accurately reflect the oxygen consumption characteristics of different quality coals, providing more substantial support for assessing the spontaneous combustion risk in goaf and preventing spontaneous combustion.

(2) Through the analysis of measured data on the variation of airflow velocity along the 1304 working face and the intake and return airways, it has been confirmed that there is air leakage communication between the 1304 working face and the overlying old goaf. The characteristics of the "three zones of spontaneous combustion" in the 13th coal seam of the lower part of the west-third lower mining area were identified by conducting CFD simulations on the flow

field in the goaf. The inert zone's boundary was 176 m away from the working face, and a comparison with field-measured data validated the accuracy of goaf spontaneous combustion oxidation zone delineation.

(3) The minimum safe advancing rate for the 1304 working face has been determined to be 1.86 m/d. With the current working face advancing rate of 9.6 m/d, spontaneous combustion in the goaf has no risk.

FUNDING

This research was supported by the National Key Research and Development Program (grant no. 2018YFC0807901) and the National Natural Science Foundation of China (grant no. 51774170). Thanks to Yan Liu from the Key Laboratory of Mine Thermodynamic Disasters and Control for her meticulous proofreading work on the initial draft of the paper.

CONFLICT OF INTEREST

The authors of this work declare that they have no conflicts of interest.

REFERENCES

1. Song, Z.Y. and Kuenzer, C., *Int. J. Coal Geol.,* 2014, vol. 133, p. 72. https://doi.org/10.1016/j.coal.2014.09.004
2. Li, L., Liu, T.T., Li, Z.Q., Chen, X.J., Wang, L., and Feng, S.L., *Energies,* 2023, vol. 16, no. 7. https://doi.org/10.3390/en16073168
3. Stracher, G.B. and Taylor, T.P., *Int. J. Coal Geol.,* 2004, vol. 59, p. 7. https://doi.org/10.1016/j.coal.2003.03.002
4. Kong, B., Li, Z.H., Yang, Y.L., Liu, Z., and Yan, D.C., *Environ. Sci. Pollut. Res.,* 2017, vol. 24, p. 23453. https://doi.org/10.1007/s11356-017-0209-6
5. Yan, H.W., Nie, B.S., Liu, P.J., Chen, Z.Y., Yin, F.F., Gong, J., Lin, S.S., Wang, X.T., Kong, F.B., and Hou, Y.N., *Thermochim. Acta,* 2022, vol. 717, p. 179345. https://doi.org/10.1016/j.tca.2022.179345
6. Guo, Q., Ren, W.X., and Lu, W., *Environ. Sci. Pollut. Res.,* 2023, vol. 30, p. 4733. https://doi.org/10.1007/s11356-022-22528-5
7. Xu, J.C., Deng, J., and Wen, H., *J. Xi'an Univ. Min.,* 1998, vol. 1, p. 14.
8. Yu, M.G., Chang, X.H., Jia, H.L., and Lu, L.X., *Coal Techon.,* 2010, vol. 35, p. 600. https://doi.org/10.13225/j.cnki.jccs.2010.04.024. Yu, M.G., Chang, X.H., Jia, H.L., and Lu, L.X., *J. China Coal Soc.,* 2010, vol. 35, p. 600. https://doi.org/10.13225/j.cnki.jccs.2010.04.024
9. Gui, X.H., Xue, H.T., Zhan, X.R., Hu, Z.Y., and Song, X.G., *ACS Omega,* 2022, vol. 7, p. 9406. https://doi.org/10.1021/acsomega.1c06703
10. Jia, X.L., Qi, Q.J., Zhao, Y.X., Zhou, X.H., and Dong, Z.W., *ACS Omega,* 2021, vol. 6, p. 8418. https://doi.org/10.1021/acsomega.1c00139
11. Hou, Z.S., Yang, S.Q., Shao, H.D., Zhou, B.Z., Cai, J.W., and Miao, J.R., *Combust. Sci. Technol.,* 2023, vol. 195, p. 2820. https://doi.org/10.1016/j.psep.2019.09.011
12. Zhang, Y.S., Niu, K., Du, W.Z., Zhang, J., Wang, H.W., and Zhang, J., *Fuel,* 2021, vol. 288, p. 119690. https://doi.org/10.1016/j.fuel.2020.119690
13. Wang, Y., Zhou, Y., Gao, J.B., Zhang, D.D., and Hao, Y., *Min. Saf. Environ.,* 2023, vol. 50, p. 97. https://doi.org/10.19835/j.issn.1008-4495.2023.01.017
14. Chen, X.K., Yang, S.X., Zhai, X.W., Wang, K., Li, K., and Hu, G.Q., *Coal Sci. Technol.,* 2014, vol. 42, p. 94. https://doi.org/10.13199/j.cnki.cst.2014.s1.068
15. Zhuo, H., Qin, B.T., Qin, Q.H., and Su, Z.W., *Process Saf. Environ.,* 2019, vol. 131, p. 246. https://doi.org/10.1016/j.psep.2019.09.011
16. Su, H.T., Zhou, F.B., Song, X.L., and Qiang, Z.Y., *Process Saf. Environ.,* 2017, vol. 111, p. 1. https://doi.org/10.1016/j.psep.2017.06.001
17. Qi, Y., Qi, Q.J., Wang, W., and Zhou, X.H., *China Saf. Sci. J.,* 2019, vol. 29, p. 120. https://doi.org/10.16265/j.cnki.issn1003-3033.2019.04.019
18. Chen, X.J., Li, L.Y., Guo, Z.B., and Chang, T.H., *Energy Sci. Eng.,* 2019, vol. 7, p. 710. https://doi.org/10.1002/ese3.287
19. Zhou, B.Z., Yang, S.Q., Wang, C.J., Hu, X.C., Song, W.X., Cai, J.W., Xu, Q., and Sang, N.W., *Fuel,* 2020, vol. 262, p. 116524. https://doi.org/10.1016/j.fuel.2019.116524
20. Gao, S.G., Gao, D.Y., Liu, Y.L., Chai, J., and Chen, J.H., *Combust. Sci. Technol.,* 2023, vol. 195, p. 1960. https://doi.org/10.1080/00102202.2021.2007893
21. He, J., Niu, S., and Chen, L., *Coal Technol.,* 2014, vol. 33, p. 54. https://doi.org/10.13301/j.cnki.ct.2014.09.019
22. Brodny, J. and Tutak, M., *J. Appl. Fluid Mech.,* 2018, vol. 11, p. 545. https://doi.org/10.18869/acadpub.jafm.73.246.27240
23. Tutak, M. and Brodny, J., *Appl. Sci.,* 2019, vol. 9, no. 24, p. 5315. https://doi.org/10.3390/app9245315
24. Gao, G.C., Li, Z.X., Zhang, C., Zhang, Y., Li, J., and Wu, B.D., *J. Saf. Environ.,* 2017, vol. 17, p. 931. https://doi.org/10.13637/j.issn.1009-6094.2017.03.023
25. Zheng, Y.N., Li, Q.Z., Zhang, G.Y., Zhao, Y., Zhu, P.F., Ma, X., and Li, X.W., *Fuel,* 2021, vol. 283, p. 118905. https://doi.org/10.1016/j.fuel.2020.118905
26. Li, Z.X., *China Saf. Sci. J.,* 2005, vol. 12, p. 85. https://doi.org/10.16265/j.cnki.issn1003-3033.2005.12.020
27. Deng, J., Zhao, J.Y., Zhang, Y.N., Huang, A.C., Liu, X.R., Zhai, X.W., and Wang, C.P., *Process Saf. Environ.,* 2016, vol. 104, p. 218. https://doi.org/10.10 16/j.psep.2016.09.007
28. Li, Z.X., Liu, Y., Jia, J.Z., Wu, B.D., and Li, H.T., *J. China Univ. Min. Technol.,* 2017, vol. 46, p. 273. https://doi.org/10.13247/j.cnki.jcumt.000643
29. Wang, H.H., Dlugogorski, B.Z., and Kennedy, E.M., *Prog. Energy Combust. Sci.,* 2003, vol. 29, p. 487. https://doi.org/10.1016/S0360-1285(03)00042-X

30. Wang, H.H., Dlugogorski, B.Z., and Kennedy, E.M., *Combust. Sci. Technol.,* 2002, vol. 174, p. 147. https://doi.org/10.1080/00102200290021416

31. Hu, D.J. and Li, Z.X., *PLoS One,* 2022, vol. 17, p. e0267631. https://doi.org/10.1371/journal.pone.0267631

32. Liu, Q., Lin, B.Q., Zhou, Y., and Li, Y.J., *Environ. Earth Sci.,* 2022, vol. 81, no. 7, p. 214. https://doi.org/10.1007/s12665-022-10329-5

33. Fan, H.D., Luo, F., Gao, S., Li, M., Lv, Z., and Sun, G., *World J. Eng.,* 2023, vol. 21, no. 3. https://doi.org/10.1108/WJE-11-2022-0470

34. Hao, M., Li, Y.L., Song, X.L., Kang, J.H., Su, H.T., and Zhou, F.B., *Environ. Earth Sci.,* 2019, vol. 78, p. 39. https://doi.org/10.1007/s12665-018-8010-5